OCULAR ULTRAVIOLET EFFECTS

FROM 295 nm TO 335 nm

IN THE RABBIT EYE

University of Houston
College of Optometry
Houston, Texas 77004

Contract No. CDC-99-74-12

U. S. DEPARTMENT OF HEALTH, EDUCATION, AND WELFARE
Public Health Service
Center for Disease Control
National Institute for Occupational Safety and Health
Division of Biomedical and Behavioral Science
Cincinnati, Ohio 45226

October 1976

The contents of this report are reproduced herein as received from the contractor. The opinions, findings, and conclusions expressed are not necessarily those of the National Insitutue for Occupational Safety and Health. Mention of trade names or commercial products does not constitute endorsement or recommendation for use by the National Institute for Occupational Safety and Health.

Donald Graves Pitts, Ph.D.
Anthony Peter Cullen, M.Sc. (Ophth)
Principal Investigators

Wordie H. Parr, Ph.D.
NIOSH Project Officer

DHEW (NIOSH) Publication No. 77-130

ABSTRACT

A 5000 watt Xe-Hg source and a double monochromator were used to produce 6.6 nm full band-pass ultraviolet radiation. Pigmented rabbit eyes were exposed to the 6.6 nm band-pass ultraviolet radiant energy in 5 nm steps from 295 nm to 320 nm and at random intervals above 320 nm. Corneal and lenticular damage was assessed and classified with a biomicroscope. A detailed description of normal variations of the rabbit eye is provided. Corneal threshold radiant exposure H_C rose very rapidly from 0.022 Jcm^{-2} at 300 nm to 10.99 Jcm^{-2} at 335 nm. Radiant exposures exceeding 2 x H_C resulted in irreversible corneal damage. Lenticular damage was limited to wavebands above 295 nm. There was an action spectrum for the lens which began at 295 nm and extended to about 315 nm. Permanent lenticular damage occurred at radiant exposure levels approximately twice the threshold for lenticular radiant exposure. The importance of establishing both corneal and lenticular damage criteria is emphasized.

ACKNOWLEDGMENTS

The authors wish to express their appreciation to Dr. Wordie H. Parr for his assistance in the direction and scope of the research accomplished under this contract. Dr. Parr's contracts with other research laboratories have aided materially in the research protocol and data evaluation. Pierrette Dayhaw Hacker, Ph.D. has provided assistance in animal care, animal exposures to ultraviolet, and histological techniques to be used in completion of the study. We thank her for her assistance in accomplishing the goals of the research effort.

CONTENTS

OCULAR ULTRAVIOLET EFFECTS

FROM

295 nm TO 335 nm

INTRODUCTION

The purpose of the research was to establish the effects of ultraviolet (UV) radiation on the eye in the 295 nm to 400 nm wavelength range and to provide data from which protective criteria and effective standards may be established. This report includes results only through 335 nm.

There is little quantitative research data available which may be used to establish the ocular effects of exposure to the near UV spectrum between 300 nm and 400 nm. A review of the pertinent literature is presented to demonstrate the need for research in this area of the UV spectrum.

Verhoeff *et al.*[1] used a quartz mercury lamp operating at 3.5 A and 90 V across the terminals of the tube. The lamp produced 65% of the total radiant flux in the UV range. At 59 cm from the lamp, the total abiotic irradiance was 4.2×10^{-4} Wcm^{-2} of which 2.1×10^{-4} Wcm^{-2} was above 295 nm. It was stated that 3 minutes provided a liminal exposure. Verhoeff's threshold exposure for wavelengths greater than 295 nm was 3.78×10^{-2} Jcm^{-2} radiant exposure for the rabbit cornea. It is interesting to note that with exposures below 5 minutes (6.3×10^{-2} Jcm^{-2}) Verhoeff does not describe lenticular changes. All exposures of 5 minutes or greater are described as showing abiotic changes in the

lens epithelium in as little as 24 to 48 hours. The lenses showed marked changes in the epithelium and the lens substance was affected, but only at a depth of about 20 μm beneath the capsule. Lens epithelial changes reached their maximum in 48 to 72 hours and included swelling of cells, appearances of granules in the cytoplasm, and the formation of a peripheral wall of cells. The peripheral wall consisted of a ring of deeply staining cells at the periphery of the exposed area. The nuclei of the lens epithelium cells remained normal, in spite of the above signs, except with intense exposures.

At 10 to 12 days after exposure, the lens epithelial cells lost their swollen appearance and the granules almost entirely disappeared. The nuclei were of various sizes and shapes rather than the usually observed constant size. These capsular changes persisted up to 2 months after exposure. It is interesting that Verhoeff does not give information on changes in the lens substance which would result in lenticular opacities.

An important but often ignored finding of Verhoeff's study was that the corneal endothelium was destroyed when exposed to wavelengths longer than 295 nm for 6 to 12 minutes. The corresponding radiant exposure would be 7.56×10^{-2} Jcm^{-2} and 15.2×10^{-2} Jcm^{-2}, respectively. Loss of the endothelium resulted in a marked swelling of the corneal stroma reported to be as much as 200%. The endothelium may be the key to threshold damage to ultraviolet above 295 nm.

Trümpy[2] exposed rabbit eyes to UV wavelengths from 280 to 435 nm but did not provide calibration data on his source. He observed qualitative lenticular changes which could not be compared to previous data. van der Hoeve[3] criticized the research of Trümpy and compared Trümpy's work with previous data.

The cited references by van der Hoeve will not assist materially in quantifying the radiant exposure threshold of UV in the 300 to 400 nm waveband range.

Fischer et al.[4] used narrow bandwidth UV from 250 to 350 nm and observed a change in the reflex-image of the cornea. They established 4.5×10^{-1} Jcm^{-2} as the threshold at 350 nm for the rabbit. The source was either a carbon arc or a tungsten strip-lamp passed through a double monochromator. A thermopile was used for calibration purposes. The irradiance varied from 0.2 to 2.0 Wcm^{-2} and the duration of exposures varied from 2 to 60 minutes. Fischer et al. do not provide a sufficient description of their observations to determine if the exposures above 300 nm can actually be compared with other data. They did not use a biomicroscope to observe lenticular and aqueous changes.

Bachem[5], using a filtered UV spectrum, concluded that exposure to repeated high dosages of longer UV wavelengths can cause cataracts through cumulative effect. He reported that the action spectrum for cataracts begins abruptly between 293 and 297 nm, reaches a peak near 297 nm, and falls abruptly near 313 nm. Minimal effects exist through the remainder of the near UV. In both the rabbit and guinea pig, reversible lenticular "blurring" occurred 5 to 10 days after exposure. With repeated "excessive" exposures to the 297 to 365 nm waveband, irreversible lenticular opacities occurred after a latency period which varied between 2.5 to 15 months. Bachem presents in tabular form the threshold values for lenticular opacity in the rabbit. While a bandwidth with 254 nm predominating was unable to produce a lenticular opacity, a waveband containing 297 nm and 289+ nm (he doesn't say + what) required 2.0×10^{-1} Jcm^{-2} total exposure to produce a lenticular opacity. A waveband containing ultraviolet only

above 302 nm, but not further defined, required a 1.5×10^{1} Jcm^{-2} total exposure. Finally, the spectral range from 334 to 365 nm required 5.0×10^{3} Jcm^{-2} radiant exposure to produce an opacity. Bachem concludes that daylight contains none of the far ultraviolet and far infrared and, since both the visible and near infrared are freely transmitted by the ocular media, it would appear that the near ultraviolet was responsible for cataracts.

Bachem's threshold dosage in Jcm^{-2} was as follows:

Reaction	Containing 297-289+ nm	Only above 302 nm	334-365 nm only
Rabbit lens, opacity	2.0×10^{-1}	1.5×10^{1}	5.0×10^{3}
Guinea-pig lens, opacity	1.0×10^{-1}	1.0×10^{1}	5.0×10^{3}
Guinea-pig, lens cataracts	3.0×10^{-1}	*4.0×10^{1}	3.0×10^{4}

* Cumulative from repeated applications

It is evident from the variability of the above-cited research that a threshold value for the 300 to 400 nm spectral range has not been established. Verhoeff et al. arrived at 6.3×10^{-2} Jcm^{-2} radiant exposure for wavelengths above 295 nm while Fischer et al. found a 4.5×10^{-1} Jcm^{-2} threshold at 350 nm. Both research groups used different criteria and it appears that Verhoeff et al. actually produced lenticular and endothelial damage while Fischer's group demonstrated only corneal damage. In contrast, Bachem found a threshold of 1.5×10^{1} Jcm^{-2} for the waveband above 302 nm and 5.0×10^{-1} Jcm^{-2} for the 334-365 nm waveband range. Bachem's observations are based on a minimal number of positive findings and, therefore, the validity of his threshold values may be open to question.

Cloud et al.[6] found that methoxsalen fed or injected into guinea pigs or mice sensitized their ocular tissues to damage by subsequent exposure to "black light". The skin of the eyelid was eroded and the cornea was edematous. Anterior cortical lenticular opacities developed within 5 months after a 24-hour exposure and were the only significant observed changes after a chronic exposure of 10 minutes a day for 6 days a week for up to 5 months duration. Cloud et al. do not provide the radiant emittance of the source and were interested only in the gross changes since histologic observations were not reported.

Clark et al.[7] and Lerman[8] reported that the level of the insoluble protein albuminoid in the normal human crystalline lens increases from a low of about 3% below the age of 10 to about 40% at the age of 80 to 89 (Table I). This level of insoluble protein increases to about 70% for the human lens nucleus with advanced brunescent and nigrescent nuclear cataracts. There was also a large decrease in the concentration of the smaller γ-crystalline protein, a small decrease in β-crystalline protein and an increase in the large α-crystalline protein.

Lerman's research indicated that the activation spectrum of γ-crystalline was well within the UV absorption spectra of purified fluorogen. Fluorogen shows a maximum absorption at 278 nm, a small absorption at 305 nm, and a fairly significant absorption peak at 370 nm. It is well known that the lens fluorescence increases as the human becomes older. Lerman hypothesizes that the fluorescent material could be derived from tyrosine or tryptophan which are residues in the γ-crystalline molecule. Further, the fluorogen could be formed by a photooxidation process from UV light between 340 and 380 nm. This

TABLE I

Age-Related Soluble and Insoluble Protein Fractions in Human Lenses (After Clark et al.[7] and Lerman[8])

Age (years)	Soluble protein (%)	Insoluble protein (%)	Average weight of lens (gm)
0-9	96.7	3.3	0.1167
10-19	97.1	2.9	0.1484
40-49	96.7	3.3	0.2130
50-59	90.9	9.1	0.2096
60-69	84.3	15.7	0.1840
70-79	82.6	17.4	0.2246
80-89	60.1	39.9	0.2328
	Brunescent and Nigricant Cataracts		
70-90	29.0	71.0	0.2255

TABLE II

Age-Related Changes in α-, β-, and γ-Crystalline Concentrations

(After Clark *et al.*[7] and Lerman[8])

Species and Age	α-Crystalline (%)	β-Crystalline (%)	γ-Crystalline (%)
Human			
10-19 years	37	38	25
60-69 years	55	33.6	11.4
80-89 years	57.6	33.7	8.7
Rat			
5-6 weeks	20	20	60
6 months	38	42	20
11 months	41	46	13

spectral band of UV is readily transmitted by the cornea and aqueous and readily absorbed by the crystalline lens (Figure 1). Lerman further states that the S-S linkages and the C-S linkages are involved in the formation of the albuminoid fraction. He postulates that fluorogen polymerization and decreased solubility add to some of the urea-insoluble albuminoid fraction.

Pirie[9] and van Heyningen[10] feel that the whole-lens proteins are photooxidized by virtue of destruction of tryptophan groups in the protein. Pirie suggested that photooxidation probably occurs with histidine as well. van Heyningen has found free fluorescent substances in human lenses which can sensitize the photooxidation of lens protein and appear to be derived from tryptophan metabolism. Pirie's research indicates that the brown insoluble protein in cataractous human lenses may be linked to the lens proteins by fluorescent pigmented photoproducts. Kurzel, Wolbarsht, and Yamanashi[11,12] have presented evidence that tryptophan photoproducts were bound to human cataractous lens proteins by fluorescence and phosphorescence studies of the whole lens. Although products of tryptophan were identified, it was not clear whether these products were bound or a part of the peptide chain.

Zigman et al.[13] studied the chemical effects of near UV radiant exposure on tryptophan using human crystalline lenses. The source was a photochemical lamp filtered to produce a wavelength range from 340 to 380 nm with an irradiance of 3000 μWcm^{-2} and a maximum emission at 365 nm. They found that exposure of tryptophan to near UV leads to chromatic photoproducts which bind to the lens proteins, alter their color and change solubility. Human lens material without added tryptophan did not show chromatic changes on exposure to long-wavelength

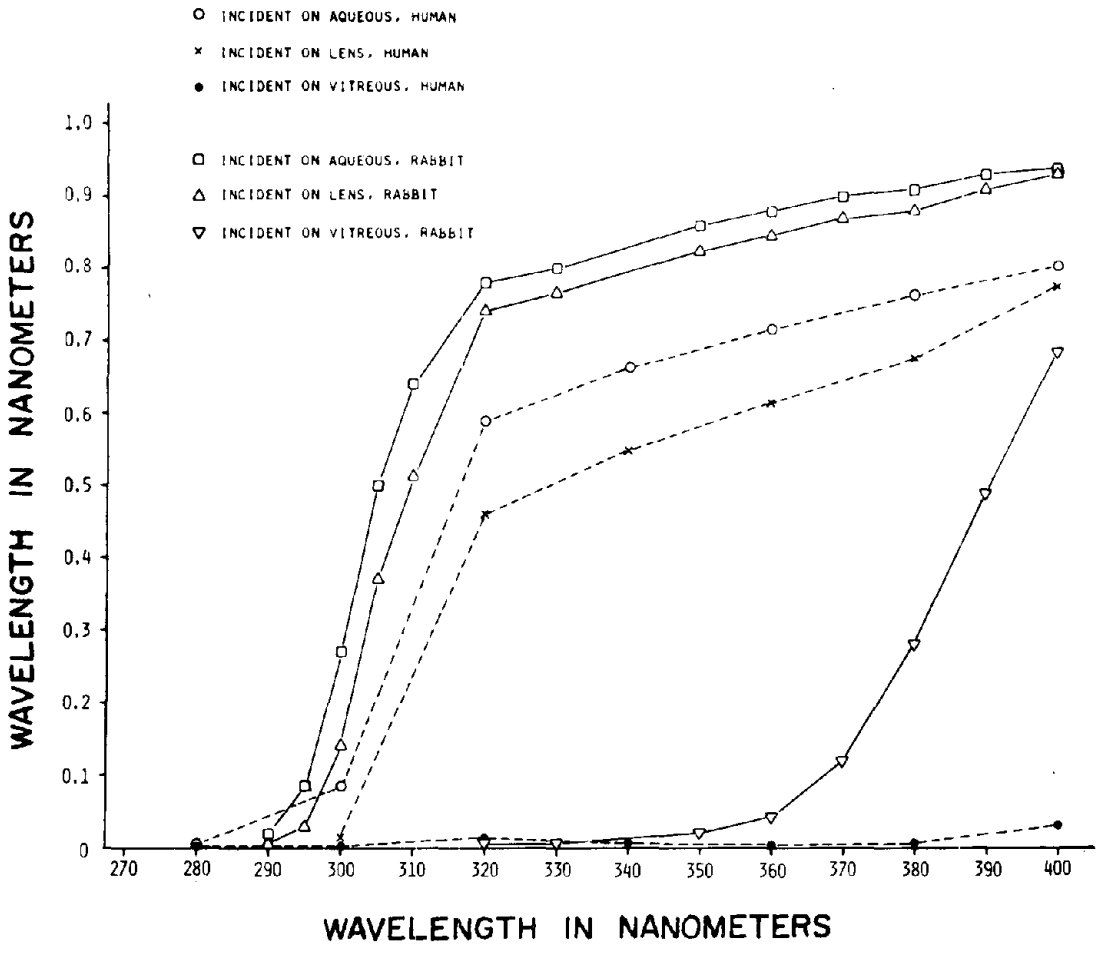

FIGURE 1. Comparison of rabbit and human transmittance of ultraviolet through the cornea, aqueous humor, crystalline lens, and incident on the vitreous. Most of the wavelengths below 300 nm are absorbed by the cornea while the wavelengths between 310 and 390 are absorbed by the lens (after Boettner and Wolter[31], Kinsey[32], and Bachem[5]).

UV until after 48 hours of exposure. Tryptophan showed an excitation wavelength at 278 nm and a fluorescent emission at 330 nm. However, following exposure to near ultraviolet, tryptophan showed an additional 360 nm excitation and 440 nm fluorescence similar to that found in the brunescent human cataract lenses.[14] The ultraviolet irradiance for these studies was 3 to 5 μWcm^{-2} at 365 nm and exposures were made for at least several hours.[15] These exposure levels exceed those expected for sunlight for the same period of time.

Zigman et al.[16] and Zigman and Vaughan[17] have continued research in the above area and shown mouse eye tissue damage for exposures of 12 hours a day up to 90 weeks. Lens epithelial cells seemed to lose their ability to differentiate into fiber cells after 35 weeks of exposure while anterior and posterior cataracts developed at 50 weeks. The retinal photoreceptors of these mice became thin, then were invaded by phagocytic wandering cells and destroyed. Photoreceptor thinning was noted by 14 weeks and total loss of the photoreceptors occurred by 70 weeks. No corneal damage was observed.

Zigman and Bagley[18] in an in vitro study of dogfish retinas have shown that RNA and protein precursor incorporation in the photoreceptors was inhibited after exposure to 3 to 4 μWcm^{-2} at 365 nm for 8 hours. They suggested that the mechanism was an inhibition of cytochrome activity which had been shown previously to be sensitive to blue and near UV exposure.

In an attempt to determine the role of near UV in the production of cataracts, Zigman et al.[19] studied in vitro dogfish lenses and exposed mice to a near UV environment. Freshly enucleated dogfish lenses were prepared and incubated with a 320 to 380 nm bandwidth ultraviolet source with an irradiance of

3000 μWcm^{-2} for 24 hours prior to biochemical evaluation. The mice were reared in a controlled near UV environment which ranged in irradiance from 200 μWcm^{-2} to 600 μWcm^{-2} at 365 nm. At 6- to 7-week intervals, the mice were sacrificed for histologic and biochemical study. The mouse research showed that the *in vivo* effect of near UV was to inhibit the accumulation of soluble proteins in the lens. This could have resulted from a direct effect on the protein-synthesizing system or from the direct blockage of amino acid uptake as a result of lens capsule and fiber alterations. The mouse lenses also showed a marked increase in insoluble protein between 16 weeks and 43 weeks. Thus, it appears that near UV accelerates the aging process in mice by changing soluble crystallines into insoluble crystallines.

Zigman *et al.'s*[20] data show that there are at least two methods in which near UV exposure may alter the physical and chemical properties of the crystalline lens. Free aromatic amino acids may be photooxidized into compounds with strong binding affinities for lens proteins. Near UV may also photooxidize these same aromatic amino acids that comprise the protein. In either case, the photooxidation from near UV causes an increase in a yellow-brown coloration of the lens material. The photooxidation process is inhibited by the presence of ascorbic acid.

MacKeen, Fine, and Fine[21] exposed about 4.0-kg weanling rabbits to a Helium-Cadmium (He-Cd) laser operating at 325 nm with a power output of 15 μW and a 1.5-mm beam diameter. The power density was 0.85 Wcm^{-2} with exposure durations of 4, 6, 8, 16 or 32 minutes. The initial response observed was an edema of the corneal epithelium which occurred within the first few hours and

was reversible. All 32-minute-duration exposures (about 1632 Jcm^{-2}) showed localized anterior sub-capsular changes after three days which did not spread laterally with age. The final appearance was a division of the initial sub-capsular opacity into a large anterior cortical opacity and a small sub-capsular cataract. Adult rabbits of 9 to 11 kg body weight developed deep anterior cortical cataractous changes after a period of 6 months.

Ebbers and Sears[22] used a He-Cd UV laser and exposed 100 monkey eyes. The endpoint for corneal damage was a well-defined corneal lesion. An ED_{50} of 0.8 Jcm^{-2} was established and the corneal damage completely reversible within 24 to 48 hours. Ebbers and Sears reported that permanent lenticular cataracts were produced with a 6.5 Jcm^{-2} radiant exposure.

Zuclich and Connolly[23] reported on corneal and lenticular damage from a krypton-ion laser with continuous wave (cw) output at 350.7 nm and 356.4 nm simultaneously with an intensity ratio of ≈ 3:1, an argon-ion laser with cw output at 351.1 nm and 363.8 nm simultaneously with an intensity ratio of ≈ 1:1 and a nitrogen laser emitting at 337.1 nm with a 10 ns pulsewidth and a variable repetition rate up to 50 Hz. The nitrogen laser had a peak power of ≈ 1 megawatt. The krypton-ion laser (350.7 nm and 356.4 nm) produced corneal epithelial lesions in rhesus monkeys with a radiant exposure of approximately 70 Jcm^{-2}. The lesions developed within 12 to 24 hours and the epithelium regenerated back to normal within 48 hours. Multiple exposures with pulsewidths varying from 250 ns to 1 s and a pulse train of 30 s resulted in corneal damage threshold of 67 Jcm^{-2}. The nitrogen laser (337.1 nm) gave a corneal radiant exposure threshold of 8.4 ± 3.3 Jcm^{-2} for trains of 10 ns pulses.

The argon-ion laser (351.1 nm and 363.8 nm) with a continuous 30 s exposure gave a corneal threshold of 82 $\pm$ 3.3 Jcm^{-2}. Lenticular clouding was produced with a single 10 ns pulse with the nitrogen laser radiant exposure of 1.1 Jcm^{-2}. Immediate visible cataracts were found with two or more pulses. The threshold for lenticular cataracts with the argon-ion laser was 76 Jcm^{-2} for a 4 s exposure with a power output of 1 watt. The corneal irradiance for that exposure was 19 Wcm^{-2}. One-second exposures produced a lenticular opacity with a radiant exposure threshold of 19 $\pm$ 1.8 Jcm^{-2}. Retinal damage was reported with the krypton and argon laser but threshold determinations could not be made because of the variability between animals. Zuclich and Connolly concluded that the corneal damage was photochemical because the reciprocity relationship between pulsewidth and exposure threshold was equivalent to 67 Jcm^{-2}. However, lenticular damage did not follow the reciprocity relationship and was postulated to be thermal.

INSTRUMENTATION AND PROCEDURES

The source for the ultraviolet energy was a 5000 watt xenon-mercury high pressure lamp,* powered by a 10 kW, DC power supply regulated to ± 0.5% and capable of delivering from 0 to 80 amperes at 25 to 65 volts to the arc electrodes. (Figure 2). The lamp housing was cooled by two blowers. Adequate cooling was available except when the lamp was operated at high amperages.

The radiation from the source (Figure 2) was focused at the monochromator entrance slit by the housing optics. A 10-cm quartz enclosed water chamber was placed between the focusing lenses and the monochromator to remove the infrared radiation. The exit optical beam was focused by a quartz lens with a beam size of 1.6 cm x 1.8 cm at the plane of the cornea.

The desired UV waveband was obtained with a Model 25-100 Jarrell-Ash Czerny Turner double grating monochromator. The gratings were blazed at 300 nm and grooved with 1180 grooves per millimeter allowing an approximately 5.0 nm bandpass. Entrance, intermediate, and exit slits were set to pass a nominal full-band width of 6.6 nm. Full-band pass did not exceed 7.0 nm for all wavebands used in these experiments; therefore, all wavebands are reported as 5.0 nm. The double monochromator system was aligned with a Helium-neon laser and the wavelength counter calibrated with a mercury source.

Exposure durations were set with a Gerband electronic shutter controlled by an H-P Model 5330B preset counter. The preset counter allowed exposure durations of any desired length with millisecond accuracy.

An EG&G 580/585 radiometer was used to calibrate the UV source. The EG&G

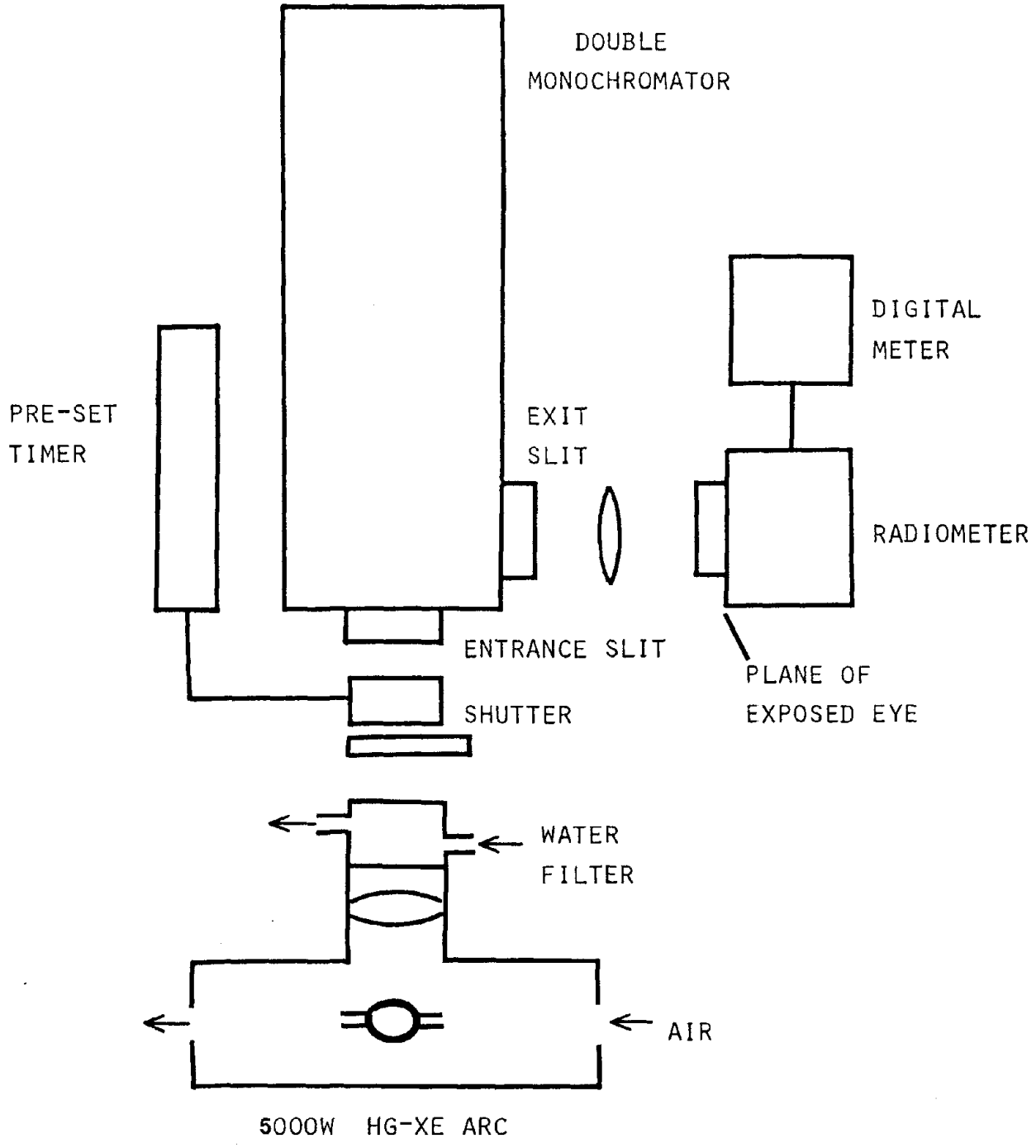

FIGURE 2. Schematic of the exposure instrumentation. See text for detailed description of the system, calibration techniques, and exposure procedures.

radiometer was cross-calibrated against an Eppley 16-junction thermopile traceable to an NBS UV standard source. The radiometer was placed in the same position that the animal's cornea would occupy.

The irradiance in Wcm^{-2} incident on the radiometer was determined by the following relationships:

$$E_{e\lambda} = \frac{ImMd}{K_{\lambda}} \qquad (1)$$

$E_{e\lambda}$ = irradiance in Wcm^{-2} for the waveband of concern

Im = current or ampere reading from the radiometer

Md = multiplying aperture

K_{λ} = radiometer calibration constant

Equation (1) was valid for the measurement of sources having a diameter equal to or larger than the aperture of the radiometer.

The radiant exposure (H) in Joules/cm^2 (Jcm^{-2}) was calculated using the following:

$$H = E_{e\lambda}T \qquad (2)$$

H = radiant exposure (Jcm^{-2})

$E_{e\lambda}$ = irradiance (Wcm^{-2})

T = exposure duration in seconds (5)

For a given irradiance $E_{e\lambda}$, the exposure duration T could be varied to obtain different values for the radiant exposure H. The exposure duration T, irradiance $E_{e\lambda}$, and radiant exposure H were determined for each animal prior to exposure using the above calibration procedure. The calibration accuracy was

estimated to be approximately $\pm$ 10%.

Prior to exposure, each eye was examined thoroughly with the biomicroscope. Any animal with anomalies of the anterior part of the eye (cornea, anterior chamber, iris, or lens) was rejected. The cornea was centered normal to the optical beam with the monochromator set at 450 nm. The eyes were exposed in 5 nm waveband steps in the wavelength range from 290 nm to 335 nm.

Ocular damage criteria are given in Table III. The criteria used to determine corneal damage were epithelial debris, epithelial stippling, epithelial granules, epithelial haze, epithelial exfoliation, stromal haze, stromal opacities and endothelial disturbances. Anterior chamber signs included flare and cells. The crystalline lens criteria were sub-capsular opacities, capsular and stromal haze, stromal opacities and increased prominance of the anterior suture. Criteria for the iris were the presence of the anterior chamber signs, changes in clarity of the iris stroma and sluggish pupillary response.

Epithelial debris may be described as small glistening bodies located in the pre-corneal tear layer. Epithelial haze is an irregular, crackled appearance of the corneal anterior surface. Epithelial granules are small, white, discrete, round spots located deep in the epithelial layer of the cornea. Epithelial exfoliation is a sloughing of layers of the epithelium. Stromal haze is a loss in the transparency or an increased scatter of the biomicroscope light from the stroma. Stromal opacities are localized areas of opacification. Endothelial disturbances include granular formations similar to the epithelial granules and keratic precipitates (KP's). Anterior chamber flare is the Tyndall scatter produced by the release of non-cellular blood components into the aqueous

Table III Ocular Ultraviolet Damage Criteria

1. Cornea

   A. Epithelium

      Discharge
      Epithelial Debris
      Epithelial Haze
      Granules
      Exfoliation

   B. Stroma

      Stromal Haze
      Stromal Opacities

   C. Endothelial Disturbance

2. Anterior Chamber

   Flare
   Cells

3. Lens

   Capsule
   Cortex
   Nucleus

4. Iris

   Stromal Haze
   Pupillary Reaction
   Posterior Synechia

of the anterior chamber. Anterior chamber cells are the release of cellular materials into the aqueous. Sub-capsular opacities are small, discrete white dots located in the anterior epithelium just beneath the capsule of the lens. Capsular and stromal haze are the result of increased scatter of the lens capsule and stroma. Stromal opacities appear to be migrations and coalescing of the sub-capsular opacities into "clumps".

Two observers independently determined the criteria status and classification of each eye. The severity of the exposure for the corneal criteria was indicated as negative (-), probably positive but not certain ($\pm$), positive (+), moderately positive (++) and severely positive (+++) and extremely positive (++++). If five or more corneal criteria were positive (+), the eye was classified as above threshold (+). Three to four positive corneal criteria were classified as threshold ($\pm$). Fewer than three positive corneal criteria resulted in a below threshold classification (-). Any lens or anterior chamber signs resulted in a positive (+) classification.

The lowest radiant exposure resulting in an above threshold classification terminated the experiment for that waveband.

Conventional statistical rounding procedures were used. All data was rounded to two significant figures. Each experimental session covered approximately 14 hours.

RESULTS

Ultraviolet exposures were made on 61 pigmented rabbit eyes during the course of this investigation which were considered valid for the report. Table IV presents the exposure data including the wavelength, animal number, irradiance, exposure duration, radiant exposure and the biomicroscopically determined classification for threshold radiant exposure. The threshold radiant exposure values for the cornea H_C and the lens H_L are summarized in Table V. The corneal threshold H_C for 300 nm and 310 nm were taken from earlier reports[23-28]. Threshold levels of radiant exposure had not been achieved at wavebands 320 nm, 335 nm and 365 nm for the lens and at wavebands 320 nm and 365 nm for the cornea. Research will continue to establish cornea and lens thresholds in the wavelength range from 295 nm to 400 nm in 5 nm waveband steps.

Figure 3 compares the ultraviolet action spectrum for the human, the primate and the rabbit.[24-29] Figure 4 presents the same data along with corneal H_C and lens H_L thresholds generated in this investigation. Table V provides a summary of both corneal and lenticular threshold radiant exposures found during this study. Figure 5 shows the corneal radiant threshold H_C and the lens radiant threshold H_L found above 295 nm and compares this data with human and primate corneal data.

In addition to the above tabular and graphic data, photobiomicroscopic pictures were taken and are used to demonstrate examples of the ocular damage in the discussion section.

TABLE IV EXPOSURE DATA

Animal Number	Irradiance $Wcm^{-2}x10^{-5}$	Exposure Duration(s)	Radiant Exposure $J\ cm^{-2}$	Classification Cornea	Lens
		WAVEBAND 295 nm			
H08R	5.5	254.	0.014	-	-
H07R	5.5	290.	0.016	-	-
H03R	15.3	105.	0.016	-	-
H05R	5.5	326.	0.018	-	-
H04L	347.8	5.18	0.018	-	-
H02R	15.9	118.	0.019	$\pm$	-
H01R	15.3	130.	0.020	H_C	-
H02L	347.8	6.32	0.022	+	-
H03L	347.8	7.19	0.025	+	-
H01L	347.8	7.48	0.026	+	-
H07L	6.7	496.	0.033	+	-
H094R	9.3	5400.	0.500	+++	-
H097R	10.22	7339.	0.750	++++	H_L
H070R	12.41	8064.	1.000	++++	+

TABLE IV EXPOSURE DATA

Animal Number	Irradiance $Wcm^{-2}x10^{-5}$	Exposure Duration(s)	Radiant Exposure J cm^{-2}	Classification Cornea	Lens
		WAVEBAND 300 nm			
H0104R	19.88	101.	0.020	-	-
H0105R	19.88	126.	0.025	-	-
H0108R	19.88	151.	0.030	-	-
H0106R	19.88	205.	0.041	-	-
H0111L	36.60	137.	0.050	H_C	-
H0110R	36.60	164.	0.060	+	-
H0109R	36.60	191.	0.070	+	-
H0112R	36.60	219.	0.080	++	-
H096R	24.14	414.	0.099	+++	-
H092R	22.70	441.	0.100	+++	-
H093R	22.70	661.	0.150	+++	H_L
H090R	24.14	828.	0.200	++++	+
H089R	24.14	1242.	0.300	++++	+
H091R	24.14	1657.	0.400	++++	+
H085L	26.80	1866.	0.500	++++	+

TABLE IV EXPOSURE DATA

Animal Number	Irradiance $Wcm^{-2}x10^{-5}$	Exposure Duration(s)	Radiant Exposure $J\ cm^{-2}$	Classification Cornea	Lens
		WAVEBAND 305 nm			
H023R	29.83	124.	0.037	-	-
H020R	31.02	129.	0.040	-	-
H016L	30.68	153.	0.047	-	-
H0117R	38.52	130.	0.050	-	-
H025R	30.68	163.	0.050	$\pm$	-
H06L	27.30	183.	0.050	$\pm$	-
H010R	26.76	231.	0.053	$\pm$	-
H08R	31.36	191.	0.059	$\pm$	-
H0123R	38.52	156.	0.060	-	-
H07R	31.36	223.	0.069	+	-
H0126L	38.52	182.	0.070	H_C	-
H012R	33.24	225.	0.075	+	-
H086R	34.10	293.	0.100	++	-
H0114L	40.57	493.	0.200	+	-
H088R	34.10	880.	0.300	+++	H_L
H0116L	40.57	986.	0.400	+++	+
H080R	32.73	1528.	0.500	++++	+
H067R	32.73	3055.	0.999	++++	+
H077R	32.73	4583.	1.500	++++	+

TABLE IV EXPOSURE DATA

Animal Number	Irradiance $Wcm^{-2}x10^{-5}$	Exposure Duration(s)	Radiant Exposure J cm^{-2}	Classification Cornea	Lens
		WAVEBAND 310 nm			
H0102R	15.33	261.	0.040	-	-
H012L	12.55	398.	0.050	-	-
H0125R	27.39	201.	0.055	H_C	-
H0104R	15.33	391.	0.060	+	-
H013R	13.29	564.	0.075	+	-
H0AL	24.78	2018.	0.500	++	-
H0101R	15.33	4892.	0.750	++	H_L
H0128L	28.88	2780.	0.801	++	+
H0115R	27.72	3247.	0.900	+++	+
H0BL	24.78	4036.	1.000	+++	+
H0CR	24.78	6053.	1.500	++++	+

TABLE IV EXPOSURE DATA

Animal Number	Irradiance $Wcm^{-2}x10^{-5}$	Exposure Duration(s)	Radiant Exposure $J\ cm^{-2}$	Classification Cornea	Lens
		WAVEBAND 315 nm			
H022R	55.13	90.	0.049	-	-
H021L	55.13	109.	0.060	-	-
H029L	55.31	118.	0.065	-	-
H030L	55.31	127.	0.070	-	-
H06L	58.90	127.	0.075	$\pm$	-
H023R	57.80	135.	0.078	$\pm$	-
H033R	55.00	164.	0.090	-	-
H034R	55.00	182.	0.100	-	-
H036R	55.00	200.	0.110	-	-
H037R	59.50	1681.	1.000	-	-
H0119R	57.96	2157.	1.250	-	-
H024R	61.25	2449.	1.500	$\pm$	-
H0121R	57.96	3019.	1.750	+ to -	-
H027L	61.25	3265.	1.990	+ to -	-
H0120R	57.96	3882.	2.250	H_C	-
H0133L	61.26	4081.	2.500	+	-
H023L	61.25	4082.	2.500	+	-
H0132L	61.26	4489.	2.750	++	-

TABLE IV EXPOSURE DATA

Animal Number	Irradiance $Wcm^{-2}x10^{-5}$	Exposure Duration(s)	Radiant Exposure $J\ cm^{-2}$	Classification Cornea	Lens
		WAVEBAND 315 nm (Cont'd.)			
H031L	70.9	5642.	4.000	+++	±
H042R	70.6	6374.	4.500	+++	H_L
H029R	68.8	7267.	4.990	+++	±
H041R	70.6	7790.	5.500	+++	+
H035R	68.8	8721.	6.000	+++	+
H074L	64.1	10924.	7.000	++++	+

TABLE IV EXPOSURE DATA

Animal Number	Irradiance $Wcm^{-2}x10^{-5}$	Exposure Duration(s)	Radiant Exposure $J\ cm^{-2}$	Classification Cornea	Lens
		WAVEBAND 320 nm			
H078L	21.6	14000.	3.02	-	-
H067L	19.3	20725.	3.99	±	-
H013OR	30.2	23217.	7.00	±	-
			7.50	H_C	+(-)
H081R	22.2	36036.	8.00	+	-
		WAVEBAND 335 nm			
H011L	35.8	10800.	3.86	-	-
H047R	60.1	9983.	6.00	± to -	-
H052R	61.3	14683.	9.00	± to -	-
H056R	63.9	16435.	10.50	± to -	-
H069R	59.2	18581.	10.99	H_C	-
H054L	59.7	20100.	12.00	+	-
H087R	57.1	26290.	15.00	++	-

TABLE IV EXPOSURE DATA

Animal Number	Irradiance $Wcm^{-2}x10^{-5}$	Exposure Duration(s)	Radiant Exposure $J\ cm^{-2}$	Classification Cornea | Lens
		WAVEBAND 365 nm		
H073L	117.0	17094.	20.00	$\pm$ to - -
H075R	111.6	22007.	25.00	$\pm$ -

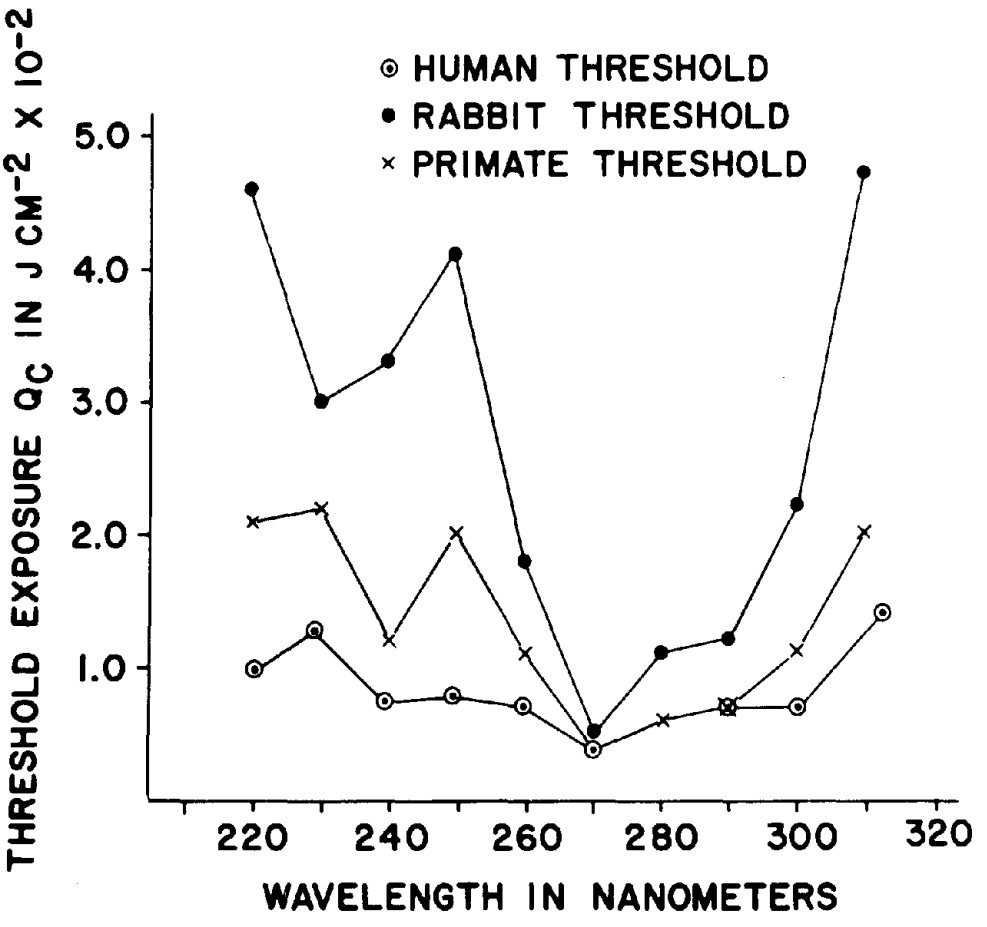

FIGURE 3. Comparison of the radiant exposure thresholds for the cornea Q_C of the human, the primate and the rabbit. The data was established by exposing 238 rabbit eyes, 83 primate eyes, and 39 human eyes to ultraviolet radiation (after Pitts[24,26]).

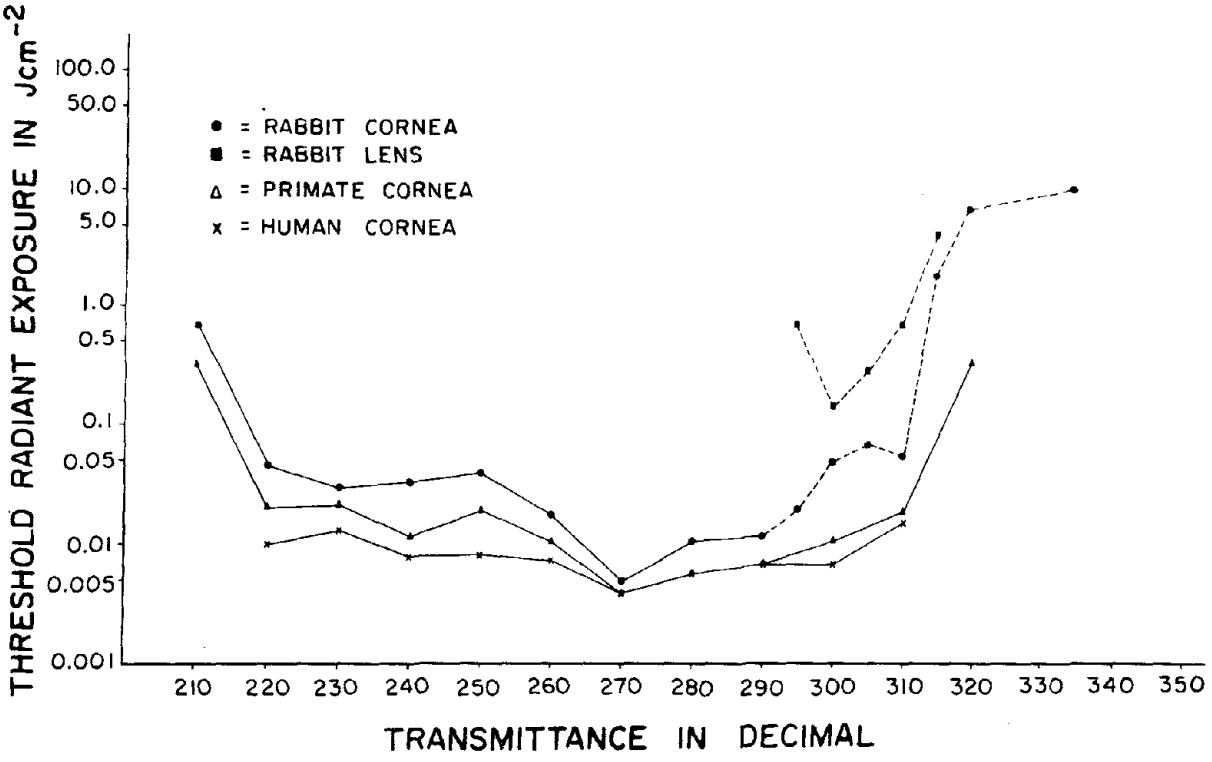

FIGURE 4. Comparison of rabbit, primate and human corneal radiant threshold with the data generated in this study. The symbols are as follows: Dotted lines represent the rabbit cornea threshold (0) and the rabbit lens threshold (□) for this study; the solid lines represent the rabbit cornea (•), the primate cornea (Δ), and the human cornea (X) thresholds.

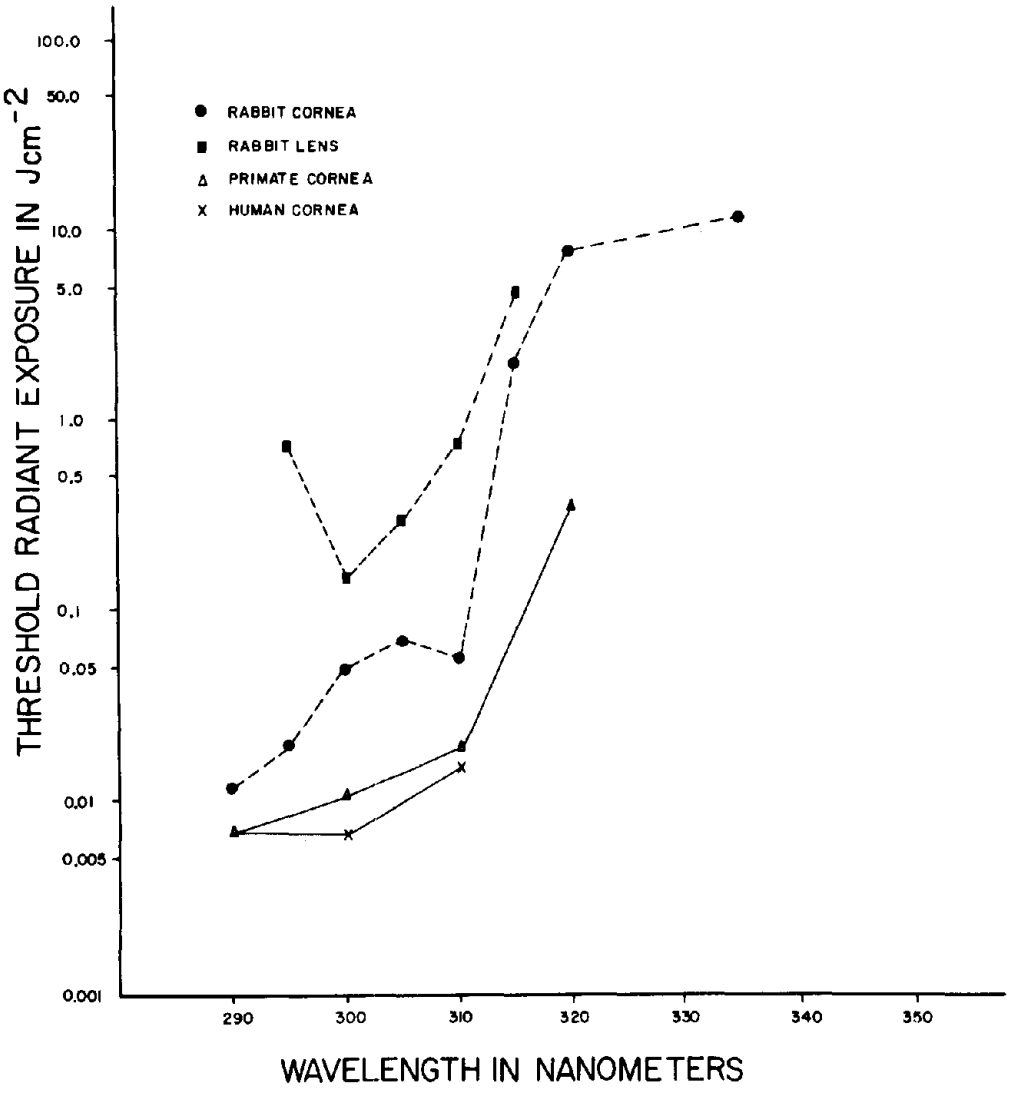

FIGURE 5. Radiant exposure for corneal and lens thresholds. The data are compared to previously established human and primate data. The symbols are as follows: dotted lines represent the rabbit cornea threshold (0) and rabbit lens threshold (□), while the solid lines represent the primate cornea threshold (Δ) and the human cornea threshold (X).

Table V Ultraviolet Threshold Data for the Rabbit Cornea and Lens

Wavelength in nm	Threshold Radiant Exposure Jcm^{-2}			Threshold Radiant Exposure Permanent Damage Jcm^{-2}	
	Corneal Threshold	Lens Threshold	Time To Disappear	Lens Threshold	Time for Permanent Damage to Appear
295	0.020	0.75	24 hrs.	1.00	2 hrs.
300	* 0.022	0.15	3 days	0.50	24 hrs.
305	0.040	0.30	7 days	0.50	24 hrs.
310	0.047	0.75	2 wks.	1.50	24 hrs.
315	0.075	4.50	1 wk.	6.00	24 hrs.
320	> 3.990	> 8.00	-----	----	-------
335	10.990	>15.00	-----	----	-------
365	>25.000	>25.00	-----	----	-------

* Taken from Pitts and Kay[24]

DISCUSSION

The biomicroscopic evaluation of normal rabbit eyes raises the question of the etiology of the long term UV induced changes described in the research literature. The "Draize System", as modified by Baldwin, McDonald and Beasley[29] was found to be inadequate for grading exposures. A detailed biomicroscopic examination of the cornea, anterior chamber, iris and lens was found to be necessary.

With increasing age, the normal rabbit's eye showed an increase in the extent and incidence of corneal farinata. Farinata are scattered dust-like opacities which occur in the corneal stroma caused by stromal condensations which increase the refractive index in small localized areas. These "normal" variations made long-term evaluation of corneal UV effects more difficult.

Another common normal biomicroscopic observation was endothelial "plaques". Endothelial "plaques" are whitish opacities of less than 1 mm in diameter located on the posterior corneal endothelial surface. The endothelial "plaques" appear and regress spontaneously without UV exposure.

Figure 6 shows an optical section of the cornea, the anterior chamber and the crystalline lens of the normal rabbit eye. The optical beam passes from right to left through the following components of the eye: A - cornea; B - anterior chamber; C - anterior capsule and anterior epithelium of the lens; D - nucleus; E - cortex; F - posterior capsule; and G - lenticular opacity. The lens nucleus D can readily be separated from the lens cortex E. Just inside the posterior capsule F is found a triangular, whitish sub-capsular cortical lenticular opacity G, with the base of the triangle resting on the posterior capsule. The

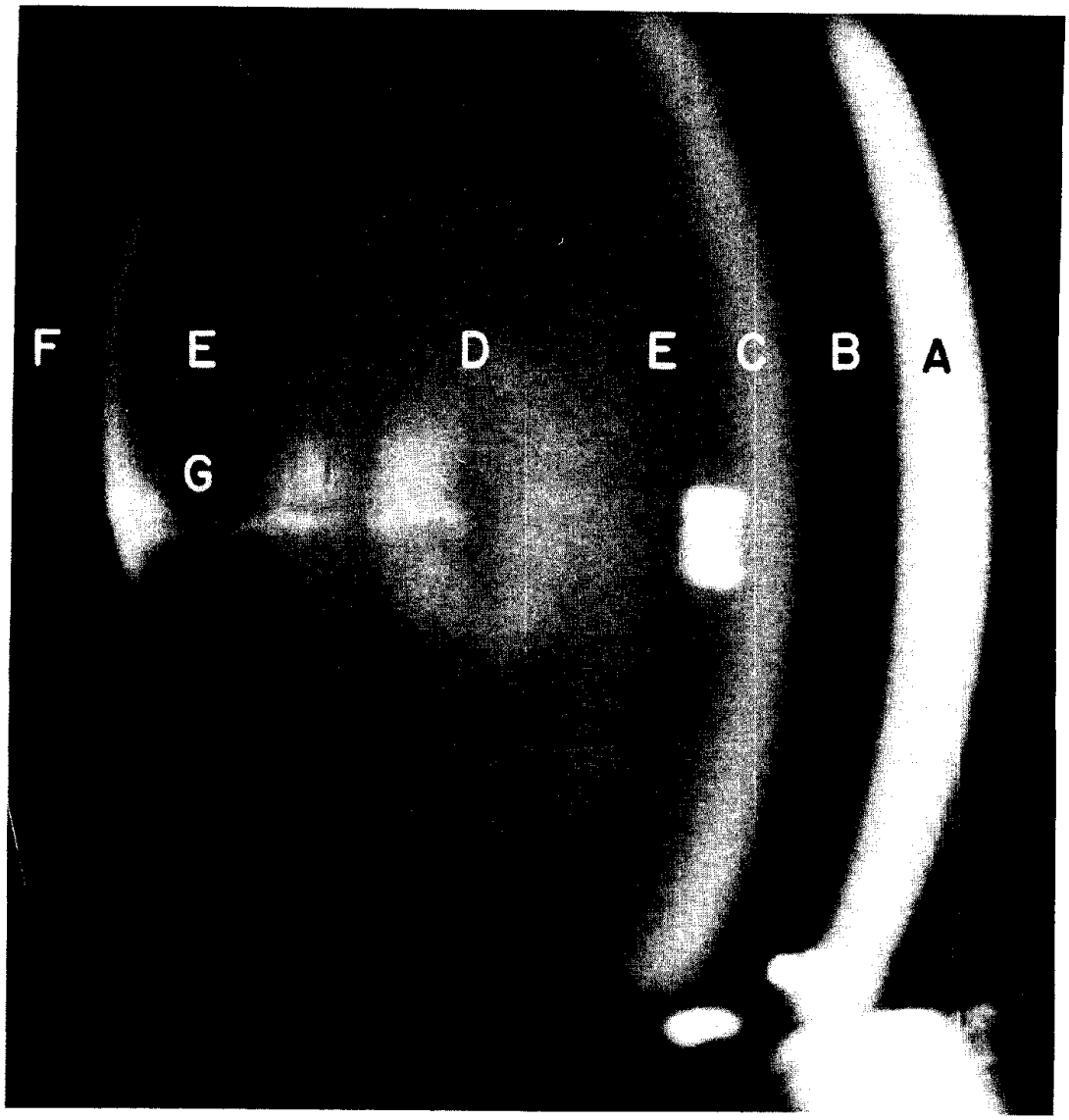

FIGURE 6. Optical section of the cornea, the anterior chamber and the crystalline lens of the normal rabbit eye. The optical beam passes from right to left through the following components of the eye: A - Cornea; B - Anterior Chamber; C - Anterior Capsule and Anterior Epithelium of the Lens; D - Lens Nucleus; E - Lens Cortex; F - Posterior Lens Capsule; and G - Lenticular Opacity. See text for detailed description.

opacity is associated with the horizontal posterior suture and extends superiorly and inferiorly along the posterior capsule F toward the equator of the lens and sends a filament anteriorly into the lens nucleus D. All animals demonstrated this posterior sub-capsular opacity just anterior to the posterior pole. The extensions of the posterior sub-capsular opacity anteriorly to the lens nucleus and along the posterior capsule toward the equator varied in extent between the different animals. Blue dot cortical cataracts were also observed in unexposed animals. Blue dot cataracts are small blue or white opacities which appear in the lens cortex. The blue dot cataract may be located in the lens cortex anteriorly, posteriorly, or towards the equator. Animals with anterior blue dot cataracts and extensive posterior polar sub-capsular cataracts were rejected.

The normal lenticular biomicroscopic findings have not been described previously in the literature. They were found in every rabbit in varying degrees. Some of the descriptions of the long-term ocular effects of ultraviolet radiation closely resemble the above biomicroscopic description of the normal rabbit eye. Therefore, it appears that a re-evaluation of the literature would be necessary for the conclusions to be valid.

Figure 5 shows the threshold radiant exposures for the rabbit cornea and lens in the 295 nm to 365 nm wavelength range. At 300 nm and above, the lens and cornea curves are relatively parallel up to about 320 nm. From the shape of the curves, it appears that the corneal and lenticular thresholds will become almost equal above 320 nm. The action spectrum for the corneal threshold extends from 210 nm to about 315 nm. This action spectrum was established from previous research and its upper limit was substantiated again in this study. The action

spectrum for the lens extends from 295 nm to at least 335 nm; however, it appears that the most effective wavelength range for producing lenticular opacities was from 295 nm to 315 nm. The most surprising finding in this study was the relatively low radiant exposures in the 295 nm to 315 nm wavelength range which were required to produce lenticular opacities. The cornea, however, would be damaged at lower radiant exposures and should provide protection against lenticular damage.

Figure 5 also compares corneal and lenticular damage in the 290 nm to 400 nm wavelength range to the previous corneal data of Pitts et al.[24,25,27] for the rabbit, primate and human corneal thresholds. Limited data above 300 nm for the human eye does not allow a detailed comparison; however, the human corneal threshold was considerably below that for either the rabbit or the primate. The primate corneal threshold was somewhat below the rabbit corneal threshold until 320 nm where little or no difference was found. The sharp rise in the lens threshold below 300 nm is probably due to the absorption characteristics of the cornea (Figure 2). Almost complete absorption of the ultraviolet radiation occurs at 290 nm and below. The radiant exposure required to produce a threshold response at 295 nm was 5 times the threshold value at 300 nm (0.75 Jcm^{-2} vs. 0.15 Jcm^{-2}), which supports establishing the lower wavelength of the lens action spectrum at 295 nm.

Corneal changes followed a rather consistent pattern of increased involvement as the radiant exposure was increased. At threshold and above, there was a consistent increase in epithelial debris. The granules observed at wavelengths between 250 nm and 300 nm, coalesced to form a network following high radiant

exposures. Epithelial damage, stippling, and haze were detected within two hours following exposure. Stromal damage, haze, and opacities appeared within 24 hours after exposure. Endothelial changes were noted within 4.5 hours after exposure. Exposures of 2 x H_C usually resulted in irreversible damage to the cornea.

Severe corneal reactions were accompanied by secondary anterior uveitis. Anterior uveitis is characterized by ciliary injection, aqueous flare, and membranous inflammatory by-products deposited on the corneal endothelium. (Figure 7). Anterior uveitis made it difficult to observe the lens or its capsule. Anterior uveitis usually regressed spontaneously within approximately two days. Table VI provides information on the wavelength, radiant exposure, time after exposure and time to recover from anterior uveitis. It is apparent from Table VI that no anterior uveitis was induced by ultraviolet radiant exposures above 315 nm.

At 295 nm, the radiant exposure required to produce a positive lenticular disturbance also produced an immediate corneal reaction with epithelial haze, granule formation, stippling, and anterior stromal haze over the entire irradi-

Table VI Anterior Uveitis

Wavelength	Radiant Exposure Jcm^{-2}	Time After Exposure	Recovery
295	0.75	1 hour	24 hours
300	0.50	24 hours	48 hours
305	0.30	24 hours	48 hours
310	1.00	2 hours	24 hours
315	No anterior uveitis found		
320	No anterior uveitis found		
335	No anterior uveitis found		

FIGURE 7. An optical section of the anterior segment of the eye which demonstrates anterior uveitis: cornea, A; membraneous inflammatory by-products on the corneal endothelium, B; and aqueous flare, C. Animal H080R, 305 nm, radiant exposure 0.5 J/cm^2, 27 hours post-exposure.

ated area. The epithelium stained extensively with sodium fluorescein confirming the immediate response. The severity of the reaction increased to complete exfoliation of the irradiated area at 20 hours post-exposure. The anterior stromal haze of the cornea also increased as the radiant exposure increased. The anterior chamber, iris, and lens were difficult to see with radiant exposures exceeding 0.75 Jcm^{-2}. Severe anterior uveitis was seen at one hour post-exposure with a radiant exposure of 0.75 Jcm^{-2}. Recovery was complete within 24 hours after exposure.

Radiant exposures above 0.3 Jcm^{-2} at 300 nm (2 x H_L) resulted in immediate corneal damage. The animal displayed extreme photophobia. Permanent damage resulted to the corneal epithelium, stroma, and endothelium. There was a thickening of the cornea and a dense posterior stromal striate. The iris was swollen with a sluggish pupillary response. The anterior chamber demonstrated a slight flare and a few cells were found in the aqueous. The cornea thickening indicated an interference with the normal metabolism of the endothelium. Minor anterior uveal changes were found at a 0.2 Jcm^{-2} radiant exposure which returned to normal within three days. Below 0.2 Jcm^{-2}, anterior uveal changes were not found.

At 305 nm, radiant exposures above 0.3 Jcm^{-2} resulted in granules, opacities, stippling and fluorescein staining of the corneal epithelium. In addition, the stroma of the cornea was hazy and developed opaque striae after about 8 days. Within 24 hours, there were severe fibrinous endothelial deposits. An aqueous flare was noted within 4 hours post-exposure but was reduced in severity within 24 hours. All signs of anterior uveal inflammation disappeared within 8 days. There was an exfoliation of iritic tissue within 24 hours after exposure at the

1.0 Jcm^{-2} radiant exposure. Below 0.3 Jcm^{-2}, no anterior uveal changes were found at 300 nm. There was a general increase in corneal damage as the radiant exposure was increased above the corneal radiant threshold of 0.04 Jcm^{-2}.

Radiant exposures of 1.5 Jcm^{-2} at 310 nm (2 x H_L) produced a very minor aqueous flare which disappeared within 48 hours (Figure 8). Permanent lenticular opacities and stromal opacities were also found at this level of radiant exposure. The endothelial disturbance resulted in a slight area of exfoliation and subsequent corneal thickening limited to the area of exfoliation. There was an increase in corneal involvement as the radiant exposure exceeded the corneal threshold value of 0.047 Jcm^{-2}.

At 315 nm, no anterior uveal or aqueous changes were found with radiant exposures up to 7.0 Jcm^{-2}. The general pattern of epithelial granules, epithelial haze, and stromal haze increased in severity as the radiant exposure increased. Fluorescein showed a generalized, diffuse staining of the epithelium.

The exposure data for 320 nm, 335 nm, and 365 nm are insufficient to draw adequate conclusions at this time.

No description of UV induced lenticular damage was available in the literature from which lenticular damage criteria could be established. The first biomicroscopic signs of lenticular damage were (1) loss or reduction of "orange-peel" appearance of the anterior capsule and (2) an increased prominance of the anterior suture line. These two biomicroscopic signs regressed to normal within 24 hours post-exposure. As the radiant exposure approached threshold, many small, discrete white dots appeared in the anterior sub-capsular epithelium of the lens (Figure 8). These anterior sub-capsular opacities appeared similar to

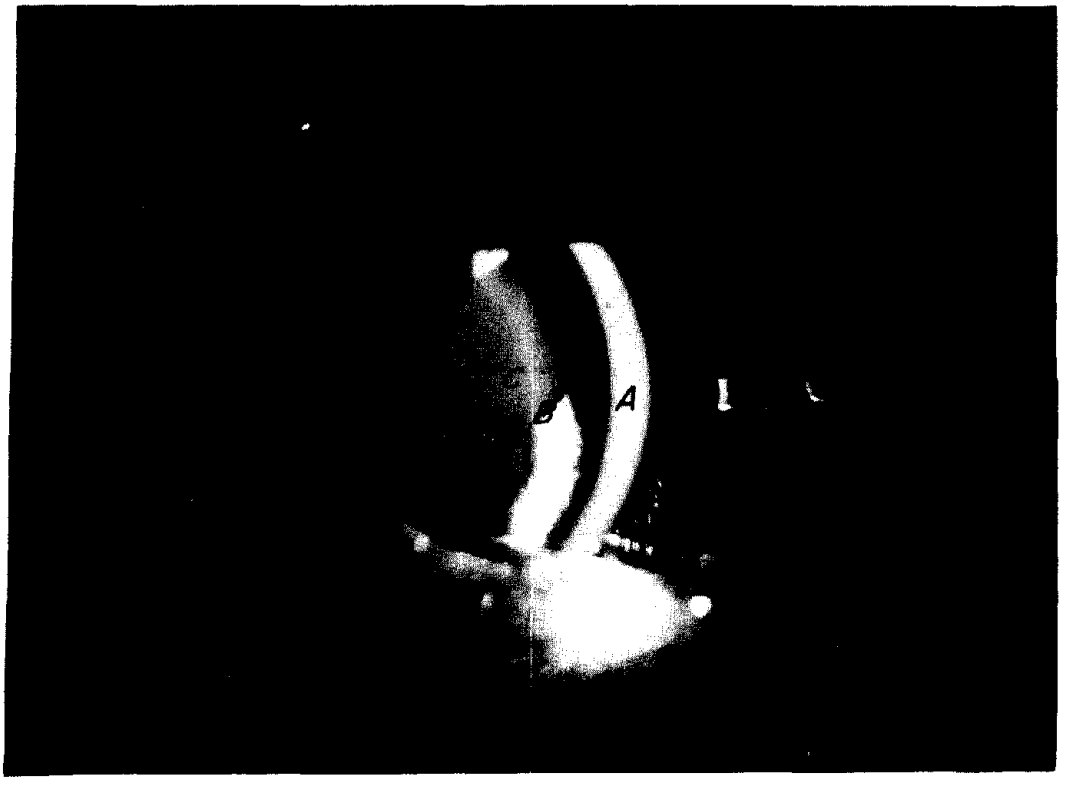

FIGURE 8. Ultraviolet lenticular damage. The optical section demonstrates the cornea, A: dot-like, discrete anterior subcapsular opacities, B; and the anterior suture line, C, a vertical whitish line bisecting the pupil. Animal HOCR, 310 nm, and 1.5 J/cm^2 radiant exposure, 24 hours post-exposure (2 x Q_L).

the corneal epithelial granules. Table VII presents the wavelength, the radiant exposure necessary to produce the lenticular opacities, the time of appearance of the lenticular opacities after exposure, and the time of disappearance of the lenticular opacities after exposure.

Supra-threshold exposures resulted in permanent lenticular opacities. The change from the small discrete white anterior sub-capsular dots into the permanent opacities developed as follows. The fine discrete opacities migrated posteriorly into the anterior cortex of the lens. An animal followed for 3 months post-exposure did not show nuclear or posterior sub-capsular opacities. At the same time, an increase in the lens stromal haze was detected. The fine opacities organized into fewer, more dense opacities. The permanent opacities usually developed in proximity to the anterior suture line. In addition to the permanent opacities, occasionally vacuoles were present. The following table presents the wavelength, radiant exposure, and the appearance of the permanent lenticular opacities following exposure. Table VIII demonstrates that permanent lenticular opacities were not induced until the radiant exposure reached $2 \times H_L$.

It was considered initially that lenticular involvement was secondary to the anterior uveitis. However, the appearance of the characteristic ultraviolet induced lens changes without and prior to the anterior uveitis negated this hypothesis.

Zuclich and Connolly [23] postulated corneal damage to be photochemical and lenticular damage to be thermal. These damage differences were based on the reciprocity relationship for corneal damage and the lack of reciprocity for

Table VII Transient Lenticular Opacities

Wavelength in nm	Radiant Exposure Jcm^{-2}	Appearance of Lens Opacities	Disappearance of Lens Opacities
295	0.75	2 hours	24 hours
300	0.15	12 hours	3 days
305	0.30	24 hours	7 days
310	0.75	24 hours	2 weeks
315	4.50	48 hours	1 week

Table VIII Permanent Lenticular Opacities

Wavelength nm	Radiant Exposure Jcm^{-2}	Appearance of Lens Opacities	Permanence* of Lens Opacities
300	0.5	24 hours	Permanent
305	0.5	24 hours	Permanent
310	1.5	24 hours	Permanent
315	6.0	24 hours	Permanent

* Lenticular opacities present one month after exposure.

lenticular damage. For example, the nitrogen laser with a wavelength at 337.1 nm produced lenticular damage at ≈ 1.1 Jcm^{-2} while the argon laser with wavelengths at 351.1 nm and 363.8 nm required 19 Jcm^{-2} for 1 second exposures and 76 Jcm^{-2} for 4 second exposures.

Table IV shows that the corneal threshold for non-coherent, long exposure ultraviolet radiation at 335 nm was 10.99 Jcm^{-2} and at 365 nm the corneal threshold was greater than 25 Jcm^{-2}. The corneal threshold of 10.99 Jcm^{-2} at 335 nm compares favorably with the nitrogen (337.1 nm) corneal threshold of 8.4 ± 3.3 Jcm^{-2}.

The data of Zuclich and Connolly show that the argon laser (351.1 nm and 363.8 nm) lenticular threshold was 76 Jcm^{-2} for a 4 second exposure and was 19 ± 1.8 Jcm^{-2} for 1 second exposures for a corneal irradiance of 19 Wcm^{-2}. These differences in responses could be due to wavelength rather than thermal. Figure 5 demonstrates the action spectra for the production of corneal and lenticular damage found in this study. The curve indicates that corneal threshold damage at 365 nm should be approximately a magnitude above the corneal threshold at 335 nm; therefore, the increased radiant exposure required to produce lenticular damage at the higher wavelengths could be due to the relative effectiveness of the 365 nm wavelength in producing a photochemical reaction rather than thermal in nature. However, the high power short duration of the laser exposures may induce thermal changes. The rate of delivery may affect damage; however, the comparison of the laser with the broadband, long duration exposures at ≈ 335 nm shows approximately the same threshold for the cornea.

It is assumed that both the corneal and lenticular damage found in this

study is photochemical. This assumption is based on the fact that the corneal and lenticular damage appeared the same as far as granules are concerned. Additionally, both corneal and lenticular damage were not obtained at threshold radiant exposure levels until after a rather long latency. Thermal damage usually occurs immediately after the tissue has been exposed. It may be that the low power, continuous, long duration exposures provided a radiant exposure which affected the lens in both a photochemical and thermal response.

The laser data appear to be in direct contrast to that of our study (Table IX).

The corneal threshold in this study at 335 nm was found to be 10.99 Jcm^{-2} and lenticular changes were not found at radiant exposures of 15 Jcm^{-2}. The characteristics of the source used in this study differs greatly from a laser source. Exposures at 335 nm were of long duration, low irradiance (10^{-4} Wcm^{-2}), the optical image falling on the cornea large (1.6 cm x 1.8 cm), and incoherent. The laser beam is essentially a single wavelength (coherent) and has an extremely small diameter. The irradiance levels produced with the laser are much higher than can be achieved with the double monochromator, high-pressure arc systems. The radiant exposure levels necessary to produce damage was achieved in less than minutes with the laser while the radiant exposure for the high-pressure system took hours. It may be that the rate of delivery has a tremendous effect in establishing the radiant exposure for a threshold response. These differences may make the comparison of laser exposures and broad-band exposures questionable. The average worker in an industrial environment would more likely be exposed to low power, large diameter, incoherent UV sources. The laser data indicate that researchers using UV wavelengths must use extreme caution.

Table IX Comparison of Monochromator Thresholds with Laser Thresholds

	Corneal Threshold	Lenticular Threshold
Pitts and Cullen	10.99 Jcm^{-2}	> 15.0 Jcm^{-2}
335 nm	Reversible Damage	
Ebbers and Sears		
He-Cd Laser	0.8 Jcm^{-2}	6.5 Jcm^{-2}
325 nm	Reversible Damage	Permanent Cataracts
MacKeen, Sears and Fine		
He-Cd Laser	-------	28.80 Jcm^{-2}
325 nm		Permanent Cataracts
Zuchlich and Connolly		
CW Krypton-ion laser	~ 60-70 Jcm^{-2}	(Retinal Lesions)
350.6 + 356.4 ≃ 1:3		
Nitrogen Laser	~ 10 Jcm^{-2}	~ 1 Jcm^{-2}
337 nm		

More recently, Ham, Mueller and Sliney[31] have reported retinal damage from the short wavelengths of the visible spectrum (488 nm, 457.8 nm and 441.6 nm) produced by the laser. They reported that the temperature rise for wavelengths below 500 nm were too small to account for the retinal lesions. Thus, the retinal damage may be induced by photochemical changes. The radiant energy necessary for threshold retinal damage was less than for longer wavelengths.

Several conclusions can be raised relative to the biochemical studies cited[8-20]. Near UV in the 300 nm to 400 nm wavelengths from the sun or artificial lights is transmitted by the cornea and maximally absorbed by the crystalline lens. Most of the research has been in vitro and on the mouse and dogfish. The corneas of these animals most probably do not possess the same transmittance characteristics as the rabbit or human cornea and, thus, could not afford the same protection against the near UV. Extrapolation of the mouse and dogfish data to higher animals may not be valid. However, studies on human cataractous lenses demonstrate that some of the biochemical changes found for certain cataracts may be equivalent to the animal studies. The human lens does absorb most of the near UV[32,33] in the 320 nm to 370 nm bandwidth which may cause photooxidation of isolated lens proteins, induce pigmentation, and an increase in cross-linking may take place.

The hypothetical nature of Lerman's[8] discussion should be realized. The implication that only gamma crystalline interaction with light or its amino acid composition would specifically lead to "fluorogen" may be misleading. Other proteins have tryptophan and tyrosine present which would have spectra similar to "fluorogen". The question of whether lens protein is directly photooxidized by

near UV, mediated by sensitizers inherent in the lens, or if free amino acids are photooxidized and bound covalently to the proteins has not been conclusively demonstrated.

Thus, biochemical research indicates that exposure of the eye to near-UV for sufficient periods of time with a low irradiance comparable to the irradiance level of sunlight may interfere with the synthesis of lens proteins, catalyze insoluble lens protein, and may result in chromatic changes in the lens. While the basic mechanism remains to be found, the evidence clearly demonstrates that both *in vitro* and *in vivo* exposure to the near UV can enhance cataractous changes in the crystalline lens.

SUMMARY AND CONCLUSIONS

A 5000 W Xe-Hg source and a double monochromator were used to produce 6.6 nm full bandpass UV radiation. Pigmented rabbit eyes were exposed to the 6.6 nm bandpass UV radiant energy in 5 nm steps from 295 nm to 320 nm and at random intervals above 320 nm. Corneal and lenticular damage was assessed and classified with a biomicroscope independently by two researchers.

The following preliminary conclusions can be drawn:

1. A detailed biomicroscopic examination of the normal rabbit eye showed corneal farinata, endothelial plaques, lenticular opacities and iris cysts. Care must be exercised when the long term evaluation of radiant energy exposure effects need to be accomplished.

2. Corneal threshold radiant exposure H_C rises very rapidly from 0.022 Jcm^{-2} at 300 nm to 10.99 Jcm^{-2} at 335 nm.

3. Radiant exposures of 2 x H_C and above result in irreversible corneal damage. Corneal damage included stromal haze, stromal opacities, endothelial changes, and a thickening of the cornea. Severe corneal damage was accompanied by secondary anterior uveitis which was characterized by ciliary injection, aqueous flare and keratic participates formed on the endothelium. Anterior uveitis was not found with exposures at 315 nm and above.

4. Lenticular damage was limited to wavebands above 295 nm. There is an action spectrum for the lens which begins at 295 nm and extends to about 315 nm. It was postulated that the absorption characteristics of the cornea was responsible for the lower wavelength cut-off.

5. The most efficient waveband for the production of lenticular damage was 300 nm which gave a radiant exposure threshold H_L of 0.15 Jcm^{-2}.

6. All threshold lenticular radiant exposures produced lenticular opacities which were transient and disappeared in 24 hours to 2 weeks post-exposure.

7. Permanent lenticular damage occurred at radiant exposure levels approximately twice the threshold lenticular radiant exposure (2 x H_L).

8. It was considered initially that lenticular involvement was secondary to anterior uveitis. The appearance of the characteristic UV induced lens changes without and prior to anterior uveitis negated this hypothesis.

9. The data demonstrate that the cornea would be damaged at lower radiant exposure levels than the lens and should provide protection against lenticular damage. However, it is important to establish both corneal and lens damage criteria in the wavelength range of 295 to 400 nm to assure that adequate protection for the worker may be provided.

REFERENCES

1. Verhoeff, F. H., L. Bell and C. B. Walker: The pathological effects of radiant energy on the eye: an experimental investigation with a systematic review of the literature. Proc. Am. Acad. Sci. 51:630-818, 1916.

2. Trümpy, E.: Experimentelle Untersuchungen über die Wirkung hochintensieven Ultravioletts and Violetts Zwischen 314 and 435.9 μμ Wellenlänge auf das Auge unter besonderer Berucksichtigung der Linse. Albrecht von Graefes. Arch. Ophthal. 115:495-514, 1925.

3. van der Hoeve, J.: Strahlen und Auge. Albrecht von Graefes. Arch. Ophth. 116:245-248, 1925.

4. Fischer, F. P., D. Vermeulen and J. G. Eymers: Uber die zue Schädigung des Auges nötige Minimalquantität von ultravioletten und infraroten Licht- Arch. f Augenheilk 109:462-467, 1935.

5. Bachem, A.: Ophthalmic ultraviolet action spectra. Am. J. Ophth. 41:969-975, 1956.

6. Cloud, T. M., R. Hakim and A. C. Griffin: Photosensitization of the eye with methoxsalen. I and II. Arch. Ophth. 64:62, 1960; 66:689, 1961.

7. Clark, R., S. Zigman and S. Lerman: Studies on the structural proteins of the human lens. Exp. Eye Res. 8:172, 1969.

8. Lerman, S.: Lens proteins and fluorescence. Isr. J. Med. Sci. 8:1583-1589, 1972.

9. Pirie, A.: The effects of sunlight on proteins of the lens, Contemporary Ophthalmology. Edited by J. Bellows. Williams & Wilkins, Baltimore, 1971.

10. van Heyningen, R.: Fluorescent compounds of the human lens, Ciba Symposium 19 (New Series). Elsevier, Amsterdam, New York, p. 151, 1973.

11. Kurzel, R. B., M. L.Wolbarsht and B. S. Yamanashi: Spectral studies on normal and cataractous intact human lenses. Exp. Eye Res. 17:65-71.

12. Kurzel, R. B., M. L. Wolbarsht, B. S. Yamanashi, G. W. Staton, and R. F. Borrman: Tryptophan excited states and cataracts in the human lens. Nature, 241:132, 1973.

13. Zigman, S., J. B. Schultz, T. Yulo and D. Grover: Effects of near-UV irradiation on lens and aqueous humor proteins. Isr. J. Med. Sci. 8:1590-1595, 1972.

14. Zigman, S.: Eye lens color: formation and function. Science 171:807, 1971.

15. Grover, D. and S. Zigman: Coloration of human lenses by near-UV photo-oxidized tryptophan. Exp. Eye Res. 13:70, 1972.

16. Zigman, S., J. Schultz and T. Yulo: Cataract induction in mice exposed to near UV light. Ophth. Res. 6:259, 1974.

17. Zigman, S. and T. Vaughan: Near UV light effects on the lenses and retinas of mice. Invest. Ophth. 13:462, 1974.

18. Zigman, S. and S. J. Bagley: Near ultraviolet light effects on dogfish retinal rods. Exp. Eye Res. 12:155, 1971.

19. Zigman, S., J. B. Schultz and T. Yulo: Possible roles of near UV light in the cataractous process. Exp. Eye Res. 15:201-208, 1973a.

20. Zigman, S., G. Griess, T. Yulo and J. Schultz: Ocular protein alterations by near UV light. Exp. Eye Res. 15:255-264, 1973b.

21. MacKeen, D., S. Fine and B. S. Fine: Production of cataracts in rabbits with an ultraviolet laser. Ophth. Res. 5:317-324, 1973.

22. Ebbers, R. W. and D. Sears: Ocular effects of a 325 nm ultraviolet laser. Am. J. Optom. and Physiol. Optics 52:216-223, 1975.

23. Zuclich, J. A. and John S. Connolly. Ocular damage induced by near ultraviolet laser radiation, Invest. Ophth., Vol. 15, (9), 760-764, 1976.

24. Pitts, D. G. and K. R. Kay: The photo-ophthalmic threshold for the rabbit. Am. J. Optom. 46:561-572, 1969.

25. Pitts, D. G.: A comparative study of the effects of ultraviolet radiation on the eye. Am. J. Optom. 47:535-546, 1970.

26. Pitts, D. G. and T. J. Tredici: The effects of ultraviolet on the eye. Am. Ind. Hyg. Assoc. J. 32:235-246, 1971.

27. Pitts, D. G.: The human ultraviolet action spectrum. Am. J. Optom. and Physiol. Optics 51:946-960, 1974.

28. Pitts, D. G. and W. D. Gibbons: Corneal light scatter measurements of ultraviolet radiant exposures. Am. J. Optom. 50:187-194, 1973.

29. Pitts, D. G.: The ocular ultraviolet action spectrum and protection criteria. Health Physics 25:559-566, 1973.

30. Baldwin, H. A., T. O. McDonald and C. H. Beasley: Slit-lamp examination of experimental animal eyes, II. grading scales and photographic evaluation of induced pathological conditions. J. Soc. Cosmet. Chem. 24: 181-195, 1973.

31. Ham, W. T. Jr., H. A. Mueller and D. H. Sliney: Retinal sensitivity to damage from short wavelength light, presented at the ARVO Atlantic Section meeting, Duke University Eye Center, Durham, N.C., November 14-15, 1975.

32. Boettner, E. A. and J. R. Wolter: Transmission of the ocular media. Invest. Ophth. 1(6):766-783, 1962.

33. Kinsey, V. E.: Spectral transmission of the eye to ultraviolet. Arch. Ophth. 39(4):508-513, 1948.

☆ U. S. GOVERNMENT PRINTING OFFICE: 1977-757-057/5734 Region No. 5-11